Joint Pathology Center
Veterinary Pathology Services

WEDNESDAY SLIDE CONFERENCE 2023-2024

Conference #13 — 13 December 2023

CASE I:

Signalment:
3-year-old intact male, Chinese-origin cynomolgus macaque (*Macaca fascicularis*)

History:
This cynomolgus macaque from a maintenance colony at a contract research organization presented for ptosis of the left eye (OS). Physical exam additionally identified mydriasis, exophthalmos, abnormal retropulsion, and ophthalmoplegia OS. Direct pupillary light reflex (PLR) was absent OS, and consensual PLR was normal in the right eye (OD); direct PLR was normal OD, and consensual PLR was absent OS. The diagnosed ophthalmoplegia OS was refractive to medical treatment, and euthanasia was elected.

Gross Pathology:
The left orbit was pale yellow. There was a firm, yellow-tan mass filling the left caudal sinuses and displacing the nasal turbinates and adjacent bone, including the orbit and ventral cranium. The ventral cranial vault was focally displaced ventrally, and there was malacia of the adjacent left temporal brain.

Microscopic Description:
Arising from the nasal turbinates and infiltrating the nasal turbinates, skeletal muscle, and surrounding bone is a densely cellular,

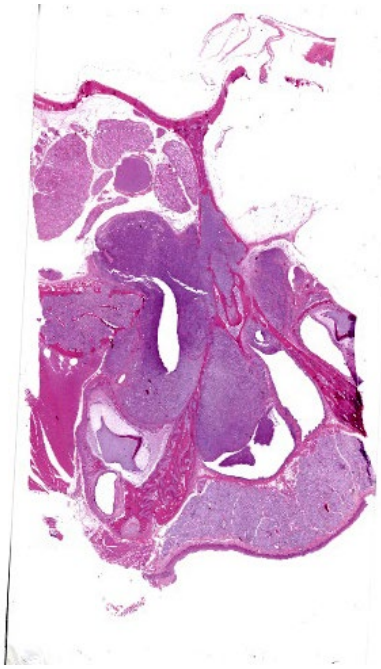

Figure 1-1. Nasal cavity, cynomolgus macaque. A densely cellular neoplasm infiltrates and effaces the bone of the nasal turbinate and maxilla and extends into the surrounding skeletal muscle. (HE, 5X)

poorly circumscribed proliferation of neoplastic cells. Neoplastic cells are arranged in nests and packets that are supported by fine fibrovascular stroma. These cells are polygonal to spindloid, have variably distinct cell borders, and contain a moderate amount of eosinophilic cytoplasm. Nuclei are ovoid to reniform, have coarsely stippled chromatin, and frequently contain 1-2 prominent nucleoli. Anisokaryosis is moderate and there are 1-3 mitoses per high power field. In areas

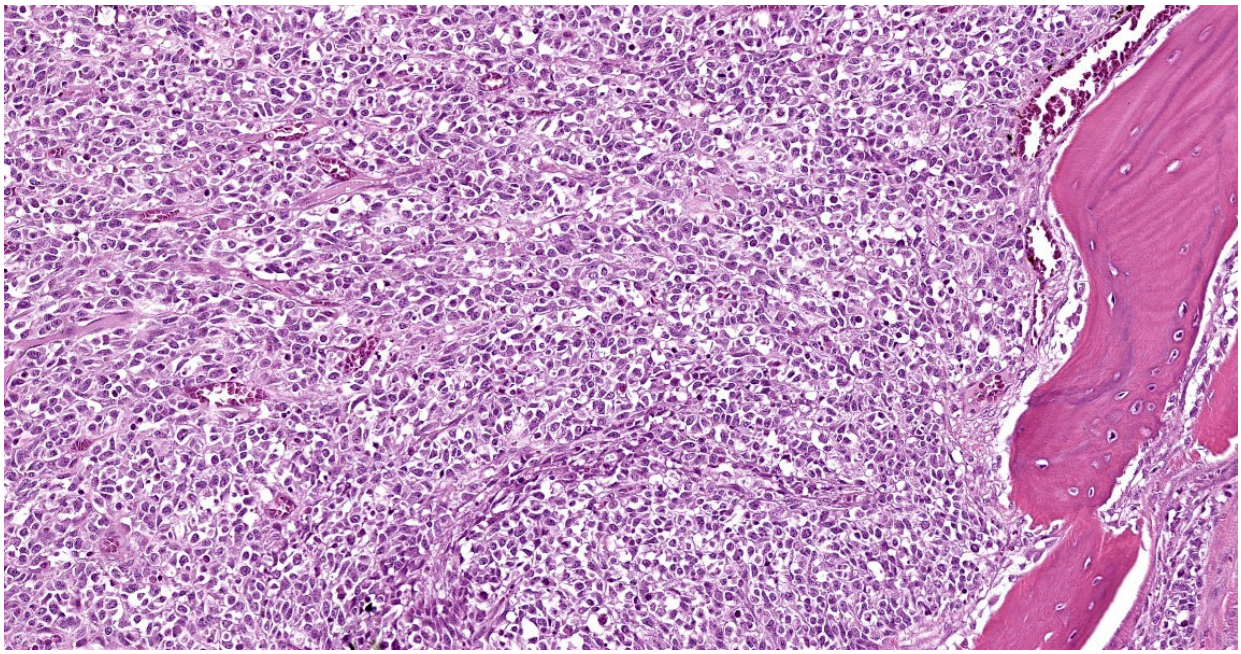

Figure 1-2. Nasal cavity, cynomolgus macaque. Neoplastic cells are arranged in nests and packets and efface the surrounding bone. (HE, 183X)

where the neoplasm extends to the overlying squamous epithelium, there is erosion and ulceration with associated hemorrhage, inflammatory infiltrates of lymphocytes, plasma cells, and neutrophils, and abundant coccoid bacteria. Neoplastic cells were not present in sections of ocular or periocular tissue, although there was degeneration and regeneration of the extraocular skeletal muscle. There is destruction of cortical and woven bone, with replacement by neoplastic cells.

Contributor's Morphologic Diagnosis:
Nasal turbinates: Esthesioneuroblastoma (Olfactory neuroblastoma).

Contributor's Comment:
Esthesioneuroblastomas are malignant neoplasms that appear histologically similar to neuroendocrine tumors. They arise from the neuroectoderm of the olfactory mucosa along the superior nasal vault. Esthesioneuroblastomas have been reported in humans, dogs, cats, horses, cows, mice, axolotls, and fish; however, they are rarely reported in cynomolgus macaques. To the authors' knowledge, this is the second report of an esthesioneuroblastoma in a cynomolgus macaque.

In the horse, literature describes neoplastic cells labelling for antibodies against neurofilament protein, synaptophysin, glial fibrillary acidic protein, neuron-specific enolase, microtube-associated protein, and S-100 protein. Microtubule-associated protein (MAP-2) has been reported to label positively in the dog, cat, and horse; however, due to the lack of specificity of immunohistochemical markers, definitive diagnosis is made by visualizing cell processes that contain microtubule neurofilaments on transmission electron microscopy. Dense core neurosecretory granules are also visualized on TEM. These neoplasms are locally aggressive and often invade through the cribriform plate and into the sinuses and brain.

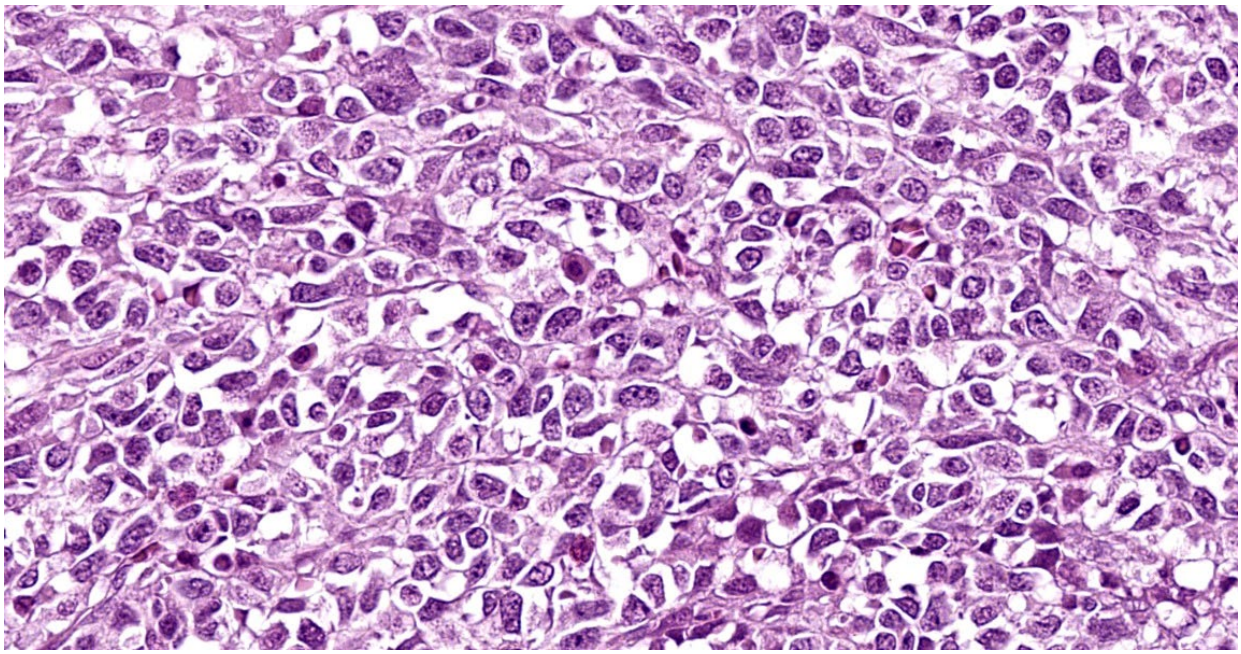

Figure 1-3. Nasal cavity, cynomolgus macaque. High magnification of neoplastic cells. (HE, 597X)

Contributing Institution:
Pathology Department
Charles River Laboratories – Mattawan
www.crl.com

JPC Diagnosis:
Nasal cavity and maxilla: Malignant neoplasm.

JPC Comment:
Esthesioneuroblastomas, also known as olfactory neuroblastomas (ONBs), are characterized histologically by epithelioid neoplastic cells with indistinct borders and scant cytoplasm that are often separated by neurofibrillary material. Rosette formation is a characteristic feature.[2] ONBs are presumed to originate from olfactory epithelium and most tumors are located in the caudal nasal cavity in close proximity to the cribriform-plate.[5] ONBs are typically invasive, leading to osteolysis of facial structures, deformation of the ethmoturbinates, and invasion into the cerebral cortex.[2,5]

Human ONBs are evaluated using a four-tiered grading scheme and case reports in veterinary medicine tend to apply this scheme to animal ONBs, though it isn't clear that this grading predicts biologic behavior in animals.[1,5] Under this rubric, grade I ONBs exhibit lobular architecture, minimal nuclear pleomorphism, prominent neurofibrillary matrix, rosette formation, no mitotic figures or necrosis, and variable amount of calcification. By contrast, grade IV ONBs have variable amounts of lobular architecture, marked nuclear pleomorphism, absent neurofibrillary matrix, occasional rosette formation, marked mitoses, prominent necrosis, and no calcification.[1]

This week's conference was moderated by Dr. Derron Alves, Chief of the Infectious Disease Pathogensis Section at the National Institute of Allergy and Infectious Diseases. Conference discussion began with a review of the microscopic anatomy of the nasal cavity and surrounding structures and the types of epithelium present in the nasal cavity.

Conference discussion focused on the seeming mismatch between the histologic appearance of ONB described in the literature and the appearance of the neoplasm on the examined slide. Participants noted the complete lack of rosette formation, the lack of neurofibrillary matrix, and the presence of respiratory epithelium with no identifiable olfactory epithelium within the examined section. An attempt was made to match the tumor to the described Grade IV ONB histomorphology, but the lack of necrosis and rosette formation did not pass the smell test. Immunohistochemical results were similarly vexing, with neoplastic cells negative, or the stains non-contributory, for the following immunohistochemical markers: NSE, NeuN, synaptophysin, chromogranin, CD3, CD20, CD138, pancytokeratin, and vimentin.

Participants had a wide range of differential diagnoses for this enigmantic tumor, including lymphoma, plasma cell tumor, round cell tumor, ONB, adenocarcinoma, and non-productive osteosarcoma. While most partipants agreed that the tumor was malignant based on the significant invasion and bony remodeling, participants felt that the histomorphology present in this section made ONB unlikely. The moderator proposed a differential diagnosis of "undifferentiated tumor, high grade," which was as specific as participants were willing to get without further investigation.

This case was referred for post-conference consultation to the soft tissue and oral and maxillofacial MD pathologists at the Joint Pathology Center, who agreed that the morphologic characteristics of the tumor were inconsistent with human ONB. They proposed an additional battery of immunohistochemical stains, to include CD45rb, desmin, ERG, MUC-1, S-100, and smooth muscle actin, to sniff out the cell of origin. These stains were performed; however the vast majority of immunohistochemical stains performed on this neoplasm were non-contributory due to inappropriate behavior of internal controls, making our immunohistochemical results, in the main, unreliable.

After multiple external consultations and a plethora of unhelpful immunohistochemistry, conference participants remained unable to ascribe a cell of origin to this inscrutable neoplasm and preferred a somewhat on-the-nose morphologic diagnosis of "malignant neoplasm."

References:

1. Brosinski K, Janik D, Polkinghorne A, von Bomhard W, Schmahl W. Olfactory neuroblastoma in dogs and cats – a histological and immunohistochemical analysis. *J Comp Path*. 2012;146:152-159.
2. Caswell JL, Williams KJ. Respiratory System. In: Maxie MG, ed. *Jubb, Kennedy, and Palmer's Pathology of Domestic Animals*. 6th ed. Vol 2. Elsevier;2016:479.
3. Lubojemska A, Borejko M, Czapiewski P, et al. Of mice and men: olfactory neuroblastoma among animals and humans. *Vet Comp Oncol*. 2014,13:70-82.
4. Meuten, DJ. *Tumors in Domestic Animals*. 5th ed. Iowa State Press;2016:473-474.
5. Siudak K, Klingler M, Schmidt MJ, Herden C. Metastasizing Esthesioneuroblastoma in a Dog. Veterinary Pathology. 2015;52(4):692-695.

CASE II:

Signalment:
4-year-old, intact male rhesus monkey (*Macaca mulatta*)

History:
The animal was experimentally infected with Simian-Human Immunodeficiency Virus (SHIV) and had a two-month history of nasal discharge and coughing and intermittent diarrhea for over a year.

Gross Pathology:
The animal is in lean body condition. Upon opening the carcass, scant adipose stores are observed. Upon opening the peritoneal cavity, the gallbladder and common bile ducts are moderately thickened. The liver is diffusely slightly pale and on cut surface the bile ducts are prominent throughout. Upon opening the pleural cavity, the lungs are mottled a pink, pale tan with a speckling of red and purple. Upon cutting through the nasal cavity, the nasal turbinates on the right side appear somewhat thickened or inflamed. Lesions are not observed in the brain, heart, kidneys, spleen, pancreas, the entire male reproductive tract, and the entire gastrointestinal tract.

Laboratory Results:
Nasal cavity swabs: *Staphylococcus aureus* (MRSA positive).
PCR on lungs: Positive for *Pneumocystis carinii.*

PCR on common bile duct: Negative for *Enterocytozoon bieneusi*; positive for *Cryptosporidium parvum*.

Microscopic Description:
Common bile duct: There is a large area of mucosal and submucosal necrosis with abun dant degenerate neutrophils and lesser macrophages. The remaining superficial mucosa

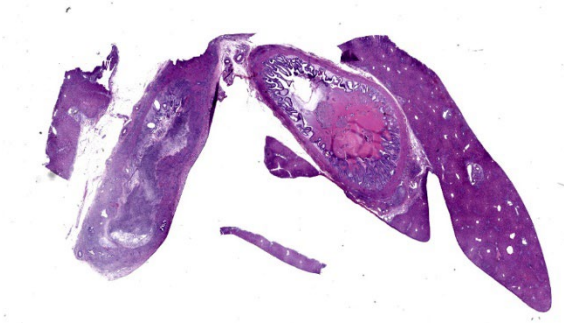

Figure 2-1. Liver, gallbladder, common bile duct, rhesus macaque. Subgross magnification of submitted tissue with (L-R): liver, common bile duct, and a second larger section of liver with gallbladder. There is partial effacement of the mucosa of the common bile duct with abundant inflammation. (HE, 5X)

is attenuated and the submucosa is edematous with abundant neutrophils, eosinophils, macrophages, and plasma cells. A few small areas of hemorrhage are observed. Areas of mucosal herniation through the muscle layers are observed. The smooth muscle has areas of atrophy and fibrosis with a mild eosinophilic and neutrophilic infiltrate. Numerous cells (smooth muscle, fibroblasts, epithelial cells) contain large basophilic intranuclear viral inclusion bodies. The mucosa has multifocal areas of 3-5 µm round protozoal organisms.

Liver: The portal areas have a mild interstitial fibrosis, mild to moderate biliary hyperplasia, a mild mixed inflammatory infiltrate, a few small areas of hepatocellular necrosis, and occasional biliary mucosal protozoal organisms.

Gallbladder: The lumen contains what appears to be a thick eosinophilic secretion admixed with mineralized and cellular debris. There are multifocal areas of submucosal edema. The mucosa has multifocal areas of protozoal organisms. The serosa has dense

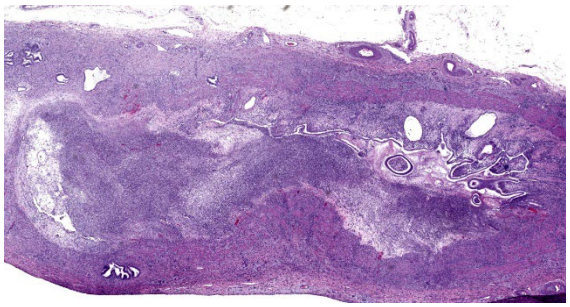

Figure 2-2. Common bile duct, rhesus macaque. There is segmental necrosis and suppurative inflammation of the wall of the common bile duct. Suppurative inflammation is present in the lumen of the duct. (HE, 19X)

areas of plump fibroblastic proliferation admixed with numerous eosinophils.

Contributor's Morphologic Diagnoses:

1. Common bile duct: Cholangitis, necrotizing, severe, with intranuclear inclusion bodies consistent with cytomegalovirus and protozoal organisms consistent with *Cryptosporidium*.
2. Liver: Hepatitis, portal, with biliary hyperplasia and *Cryptosporidium*.
3. Gallbladder: Cholecystitis, with *Cryptosporidium*.

Contributor's Comment:

This is a classic example of opportunistic infections in an immunocompromised rhesus macaque. The monkey was experimentally infected with Simian-Human Immunodeficiency Virus (SHIV). SHIV is a chimeric virus that contains HIV-1 viral envelope protein (Env) with a SIV backbone. The macaque adapted SIV (SIVmac) mirrors many of the key components of HIV-1 infection; however, there are differences between their Envs and the creation of a SIV virus with a HIV Env allows animal models to be used.[2] SHIV leads to a severe decrease in CD4 lymphocyte populations allowing opportunistic bacteria, fungi, viruses, and protozoa to cause disease.

Cytomegalovirus (CMV) is a betaherpesvirus.[1] CMV is ubiquitous in non-human primate populations. It has been identified in rhesus macaques (*Macaca mulatta*), Japanese macaques (*Macaca fuscata*), african green monkeys (*Cercopithecine aethiops*), drill monkeys (*Mandrillus leucophaeus*), squirrel monkeys (*Saimiri sciureus*), baboons (*Papio* sp.), marmosets (*Saquinus fuscicollis*, *Callithrix jacchus*), and chimpanzees (*Pan troglodytes*).[1]

In breeding colonies of rhesus macaques, 50% of infants are seropositive for CMV by 6 months of age and almost 100% are seropositive by 1 year of age. Horizontal transmission is believed to be from mother to infant through breast milk and saliva.[1] Virus is also secreted in urine, semen, and cervical secretions. In immunocompetent animals, the virus has a predilection for salivary glands.[1] In immunodeficient animals, as in human CMV, simian CMV can produce end-organ disease in the central and peripheral nervous system, lungs, lymph nodes, hepatobiliary system, gastrointestinal tract and arteries.[3]

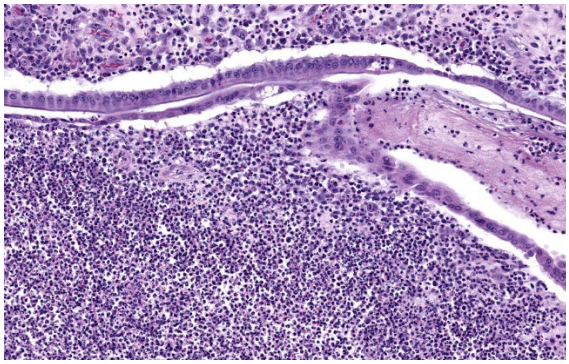

Figure 2-3. Common bile duct, rhesus macaque. There is segmental loss of the mucosal epithelium and profound suppurative and lymphocytic inflammation of the edematous lamina propria. (HE, 190X)

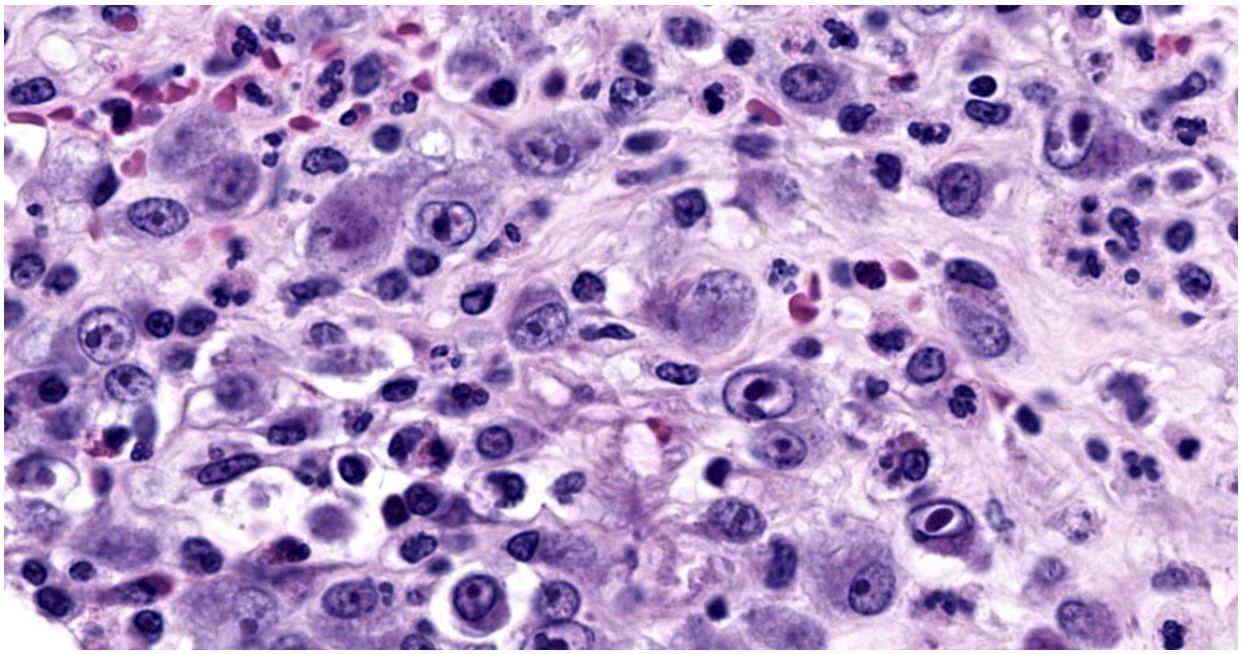

Figure 2-4. Common bile duct, rhesus macaque. Mesenchymal and inflammatory cells within the inflamed lamina propria contain karyomegalic cytomegalovirus inclusions. (HE, 881X)

CMV can be detected within multiple tissues or may be limited to a single site.[1,3]

The virus produces intranuclear (owl's eye appearance) and intracytoplasmic inclusion bodies and induces tissue necrosis and neutrophilic infiltrate in immunosuppressed animals similar to that seen in human CMV. Cells most commonly infected include fibroblasts, epithelial cells, endothelial cells, smooth muscle cells, and macrophages.[9]

Cryptosporidium is a parasitic protozoa belonging to the phylum Apicomplexa.[10] It is associated with enteric disease (diarrhea) in numerous species.[5] Animals can be infected with multiple species of *Cryptosporidium*.[10] Transmission is through the fecal-oral route and contact with animals, manure, or contaminated food and water.[5] Transmission occurs through ingestion of oocysts which release sporozoites that infect intestinal epithelial cells. The parasite then replicates asexually in an intracellular but extracytoplasmic niche present at the luminal surface of intestinal epithelial cells. Lysis of the host cell releases merozoites that reinvade other epithelial cells. After three rounds of asexual replication, obligate sexual reproduction leads to generation of more oocysts which can hatch and reinfect within the same host or be shed into feces for transmission.[4,5] In immunodeficient human hosts, infection leads to chronic disease, which can manifest as biliary involvement and sclerosing cholangitis. Cryptosporidium can also infect the respiratory tree, stomach, and pancreas.[7,11] In human AIDS, cryptosporidiosis infection increases as CD4+ T-cell numbers decrease. Restoration of these cell numbers are associated with clearance of the parasite.[4]

Hepatobiliary dysfunction is common in HIV/AIDS. AIDS cholangiopathy (AC) is a well-documented biliary syndrome in severely immunocompromised AIDS patients. AC is a syndrome of biliary obstruction and

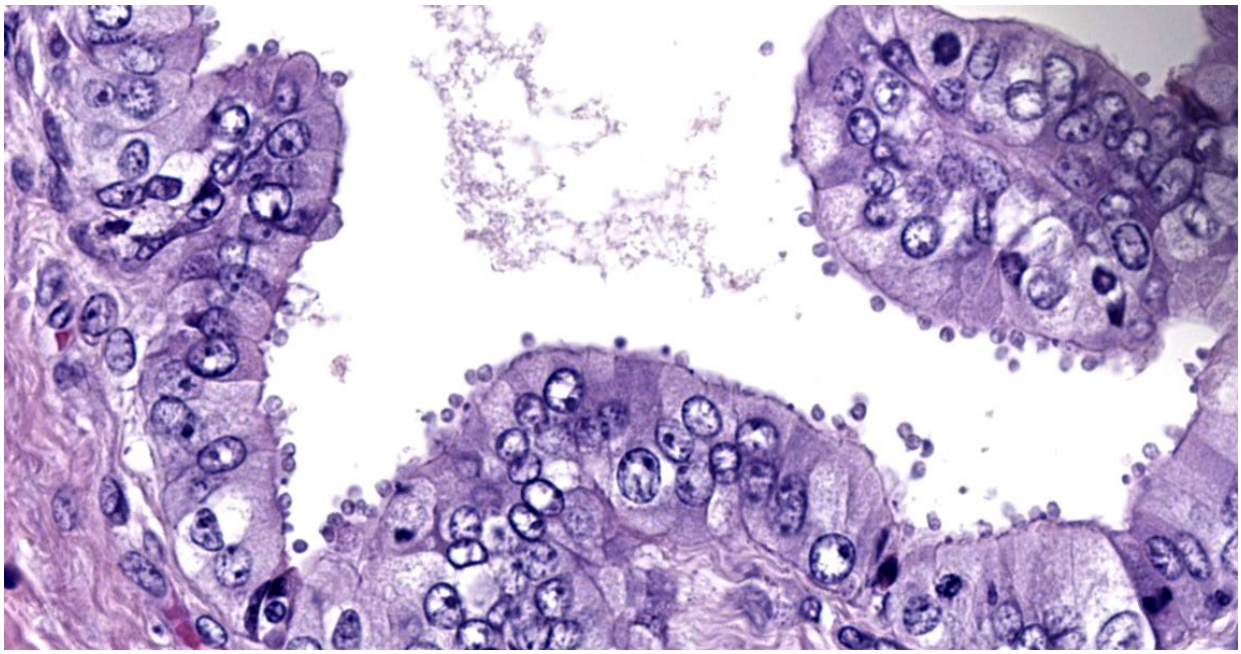

Figure 2-5. Liver, rhesus macaque. Schizonts of *Cryptosporidium* sp. are intimately attached to the epithelium lining the sublobular bile ducts. (HE, 775X)

liver damage due to infection-related strictures of the biliary tract. AC is highly associated with opportunistic infections. These infections, in decreasing prevalence, are *Cryptosporidium*, cytomegalovirus, and *Enterocytozoon bieneusi*.[6]

Contributing Institution:
National Institutes of Health
Division of Veterinary Resources
Bethesda, MD

JPC Diagnoses:
1. Common bile duct: Choledochitis, necrotizing, circumferential, chronic, diffuse, marked, with intranuclear karyomegalic viral inclusions and apicomplexan schizonts.
2. Liver, bile ducts: Cholangiohepatitis, lymphoplasmacytic and eosinophilic, chronic, multifocal, mild, with biliary hyperplasia and apicomplexan schizonts.
3. Gallbladder: Cholecystitis, lymphocytic and eosinophilic, diffuse, mild, with apicomplexan schizonts.

JPC Comment:
As the contributor notes, the pathology in this case is due to opportunistic pathogens emboldened by immunosuppression secondary to experimental SHIV infection. SHIV is a chimeric retrovirus consisting of an HIV envelope protein produced within an SIV carrier that is used for research into HIV-1 antibody-based vaccines, neutralizing antibodies, and other envelope protein-targeting strategies.

Retroviruses such as SHIV, SIV, and HIV take their family name from the presence of a reverse transcriptase within the virion that is encoded in the viral genome.[7] Reverse transcriptase is an RNA-dependent DNA polymerase that transcribes in a "reverse" fashion from RNA to DNA. All replication-competent members of the retrovirus family contain a minimum armamentarium of three major genes: *gag*, *pol*, and *env.* Reverse transcriptase is encoded by *pol* (polymerase), which also encodes the key enzyme integrase.[7] The

gag (group-specific antigen) gene encodes structural proteins and the *env* (envelope) gene encodes an envelope transmembrane glycoprotein that is broken down into a surface protein subunit (SU) and a transmembrane subunit (TM), is displayed on the virion surface, and is responsible for entry into host cells.[7] A fourth essential gene, *pro*, encodes a protease that cleaves viral precursor proteins and is expressed differently in various retroviruses.[7]

A mature retroviral virion includes a nucleocapsid containing the RNA genome and the enzymes reverse transcriptase, protease, and integrase, all of which are surrounded by an envelope studded with many SU and TM proteins. Upon encountering a host cell, the SU envelope glycoprotein makes first contact and initiates conformational changes within the TM subunit that leads to fusion of the viral and host cellular membranes and the extrusion of the nucleocapsid into the host cytoplasm. Once in the cytoplasm, reverse transcriptase co-opts the host cell replicative machinery and produces double-stranded DNA copies of the viral genome which are then integrated into random sites within the host's chromosomal DNA by the viral enzyme integrase.[7] Release of virions from the host cell typically occurs via budding from the plasma membrane.

Several retroviruses can induce oncogenesis via several mechanisms. Malignant transformation can occur when proviral DNA randomly inserts near host genes that regulate the cell cycle (proto-oncogenes). The promoter and enhancer DNA that is part of the viral insertion may result in dysregulation of the cell cycle and promote tumorigenesis.[7] It should be noted that this is a relatively rare occurrence as most viral genome integrations

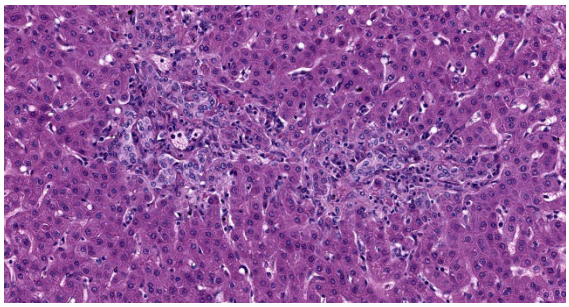

Figure 2-6. Liver, rhesus macaque. There is moderate biliary hyperplasia and mild lymphoplasmacytic pericholangitis. (HE, 250X)

are innocuous. A second method of oncogenic transformation occurs when retroviruses contain viral oncogenes. It is thought that viruses acquire these viral oncogenes from host genomes during viral recombination events; typical viral oncogenes include tyrosine kinases, growth factors, growth factor receptors, transcription factors (*v-myc*) and G proteins (*v-ras*).[7] These oncogenes are integrated into the host genome and exert strong effects on endogenous mitogenic signalling pathways, often resulting in oncogenesis. Bovine leukemia virus exemplifies a third method of oncogenesis that relies on a viral oncogene, *tax*, which upregulates both viral and host promoter sequences, no matter where on the genome *tax* is integrated (a mechanism termed trans-activation).[7]

SIV is one of many retroviruses of veterinary importance, many of which are well-studied and well-characterized. Examples include avian leukosis virus and retriculoendotheliosis virus, the oncogenic retroviruses of poultry; Jaagsiekte sheep retrovirus, enzootic nasal tumor virus, maedi-visna virus, and caprine arthritis-encephalitis virus of small ruminants; feline leukemia virus and feline immunodeficiency virus; bovine leukemia virus and bovine immunodeficiency virus; and equine infectious anemia virus.[7]

Conference discussion reviewed the SHIV animal model of HIV infection and the pathogenesis of HIV infection generally. The moderator admonished residents to remember that, while HIV famously infects and destroys CD4+ T lymphocytes, it also affects members of the monocyte-macrophage system, including microglia. Once infected, these cells secrete cytokines that ramp up the immune system, resulting in giant cell encephalitis, giant cell interstitial pneumonia, and granulmomatous lymphadenitis.

Dr. Alves drew participants' attention to the expansion of the tunica intima that was a repeatable finding throughout the vasculature in section. Arteriopathy has long been associated with SIV and HIV infection, and there have been reports of cytomegalovirus infections that manifest with intimal thickening and fibrosis with varying degrees of vasculitis. Dr. Alves could not say with certainty which, if either, of CMV or SHIV was the source of the vascular changes, but reminded conference participants not to neglect the vasculature when evaluating lesions.

References:

1. Barry PA, Chang WLW. Primate betaherpesviruses. In:Arvin A, Campadelli-Fiume G, Mocarski E, et al., eds. *Human Herpeviruses: Biology, Therapy, and Immunoprophylaxis*. Cambridge University Press; 2007:1-71.
2. Bauer AM, Bar KJ. Advances in simian-human immunodeficiency viruses for non-human primate studies of HIV prevention and cure. *Curr Opin HIV AIDS*. 2020;15(5):275-281.
3. Berg MR, Owston MA, Gauduin MC, et al. Cytomegalovirus hypophysitis in a simian immunodeficiency virus infected rhesus macaque (Macaca mulatta). *J Med Primatol*. 2017;46(6):364-367.
4. Cohn IS, Henrickson SE, Striepen B, Hunter CA. Immunity to *Cryptosporidium*; lessons from acquired and primary immunodeficiencies. *J Immunol*. 2022; 209:2261-2268.
5. Khan SM, Witola WH. Past, current, and potential treatments for cryptosporidiosis in humans and farm animals: A comprehensive review. *Front Cell Infect Microbiol*. 2023; 13:1115522.
6. Naseer M, Dailey F, Al Juboori, et al. Epidemiology, determinants, and management of AIDS cholangiopathy: a review. *World J Gastroenterol*. 2018;24(7):767-774.
7. Quinn PJ, Markey BK, Leonard FC, Fitz-Patrick ES, Fanning S, Hartigan PJ. *Veterinary Microbiology and Microbial Disease*. 2nd ed. Blackwell Publishing, Ltd.; 2011:618-634.
8. Reina FTR, Ribeiro CA, de Araujo RS, et al. Intestinal and pulmonary infection by Cryptosporidium parvum in two patients with HIV/AIDS. *Rev. Inst Med Trop Sao Paulo*. 2016;58:21-24.
9. Sinzger C, Grefte A, Platcher B, et al. Fibroblasts, epithelial cells, endothelial cells and smooth muscle cells are major target organs of human cytomegalovirus infection in lung and gastrointestinal tissue. *J Gen Virol*. 1995; 76(4):741-750.
10. Widmer G, Koster PC, Carmena D. *Cryptosporidium hominis* infections in non-human species: revisiting the concept of host specificity. *Int J Parasitol*. 2020; 50:253-262.
11. Yanai T, Chalifoux LV, Mansfield KG, et al. Pulmonary cryptosporidiosis in Simian Immunodeficiency Virus-infected rhesus macacques. *Vet Pathol*. 2000;37 (5):472-475.

CASE III:

Signalment:
14-week-old female Sprague Dawley rat (*Rattus norvegicus*)

History:
This animal gave birth with no apparent complications. At seven days post-partum, she developed paraparesis of both hind limbs. No history of trauma or mishandling was noted by the laboratory.

On physical exam, the rat was bright, alert, and responsive, euhydrated, and nursing her pups. Neurologic exam revealed absent conscious proprioception of both hind limbs, but motor reflex was intact when stimulated with a toe pinch. There was no overt pain on spinal palpation, and urination and defecation were reported to be normal. Over 48 hours, paraparesis progressed, and she lost ~7% of body weight. Euthanasia was elected due to poor prognosis.

Gross Pathology:
On necropsy, the lungs were diffusely pink with multifocal dark pink depressions and all sections floated in formalin. The heart was diffusely dark red. On cut section, a 2x5x2 mm thrombus was adhered to the right atrioventricular valve. Both kidneys were diffusely dark red and unremarkable on cut section. The spine/spinal cord appeared grossly unremarkable.

Laboratory Results:
PCR results on formalin-fixed cardiac tissue:
Corynebacterium kutscheri: Negative.
Staphylococcus aureus: Negative.
Streptococcus pneumoniae: Negative.
Group B *Streptococcus* (GBS): Positive.

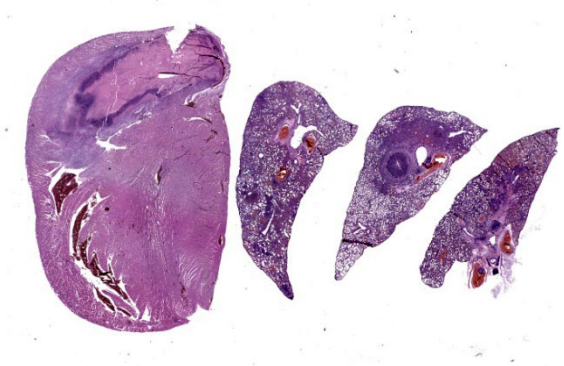

Figure 3-1. Heart and lung, rat. One section of heart and three sections of lung are submitted. At subgross magnification, a large thrombus occupies the right heart and several sections contain occlusive thrombi in the pulmonary arteries. (HE, 5X)

Microscopic Description:
Lung: Approximately 50% of small, medium, and large-caliber pulmonary vessels are distended and occluded by intralumenal abundant degenerate neutrophils, karyorrhectic debris, eosinophilic fibrillar material (fibrin), and large basophilic bacterial colonies (thrombi/thromboemboli). The elastic laminae are frequently indistinguishable, and the tunica intima, media, and adventitia are replaced by abundant degenerate neutrophils and karyorrhectic debris (necrosis). There is moderate perivascular edema and perivascular inflammation comprised of moderate numbers of neutrophils, macrophages, and lymphocytes. Occasionally, alveolar septa are expanded up to 5 times normal width by variable numbers of neutrophils, lymphocytes, and histiocytes. Bronchi/bronchioles are unremarkable.

Heart: The endocardium and right atrioventricular valve are expanded and replaced by large numbers of plump spindled cells (fibroblasts) associated with parallel capillaries within a lightly eosinophilic, fibrillar (collagenous) matrix (granulation tissue). Attached

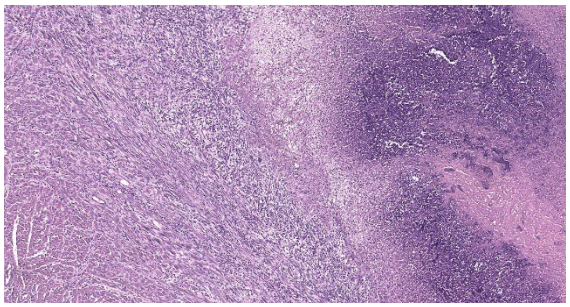

Figure 3-2. Heart, rat. The luminal thrombus is at right. The endocardium is effaced by large numbers of neutrophils, plump fibroblasts, and collagen, which extends into the adjacent myocardium (left). (HE, 125X)

to the endocardium is a thick layer of degenerative neutrophils and karyorrhectic debris with a central area of brightly eosinophilic amorphous to laminated material (thrombus) and coalescing large basophilic bacterial colonies. Infiltrating the myocardium and dissecting around myofibers are proliferating fibroblasts and multifocal mixed inflammation consisting of neutrophils, macrophages, and lymphocytes. There is mild myofiber degeneration characterized by cytoplasmic hypereosinophilia, swelling, loss of striations, and pyknotic nuclei. The epicardium is focally expanded by mild mixed mononuclear infiltrates at the apex of the heart.

Gram staining of the lung revealed abundant intravascular Gram-positive bacterial diplococci. Gram staining of the heart revealed abundant Gram-positive bacterial cocci within an atrial thrombus.

Contributor's Morphologic Diagnoses:

1. Lung: Obstructive thromboemboli, chronic, severe with necrosuppurative vasculitis/perivasculitis, and intravascular large bacterial colonies (cocci).
2. Lung: Interstitial pneumonia, chronic, multifocal to coalescing, severe, neutrophilic and lymphohistiocytic, with intralesional large bacterial colonies (cocci).
3. Heart, right atrium and AV valve: Endocarditis and myocarditis, fibrinosuppurative, chronic, regionally-extensive, severe with intralumenal thrombus, large colonies of bacterial cocci, and granulation tissue formation.

Contributor's Comment:

In addition to the right atrial thrombus and embolic bacterial pneumonia, significant microscopic findings include severe suppurative inflammation in the bladder, kidneys, and right stifle joint. Clinically noted 'paraparesis' is attributed to septic arthritis in the right stifle, though thromboemboli affecting the spinal cord or other sites is also possible.

In laboratory rodents, expected causes of prominent intralesional bacterial colonies associated with pneumonia can include *Corynebacterium*, *Streptococcus*, and *Staphylococcus* sp. Other bacterial causes of pneumonia in rats include *Pseudomonas aeruginosa* (gram-negative), *Mycoplasma pulmonis* (gram-negative), and *Filobacterium rodentium* (gram-negative).[2,3,8]

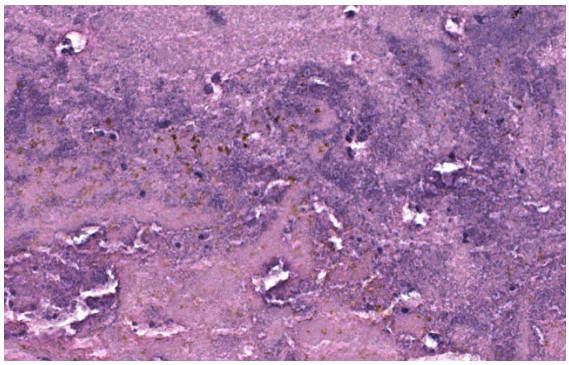

Figure 3-3. Heart, rat. There are numerous colonies of cocci within the thrombus. (HE, 580X)

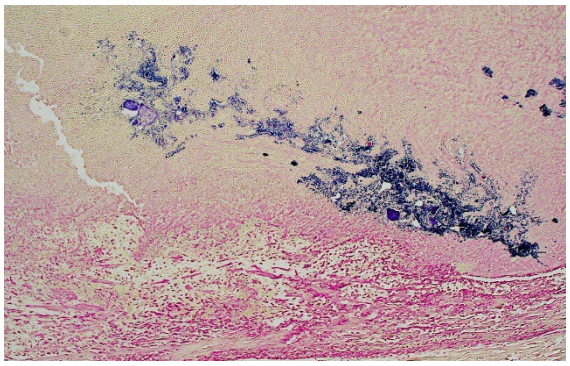

Figure 3-4. Heart, rat. Colonies of cocci within the thrombus are gram-positive. (Brown-Hopps, 100X)

Important features of this case include a prominent embolic pattern without significant involvement of the large and small airways. A major differential for bacteremia and embolic lesions in rats is *Corynebacterium kutscheri* (pseudotuberculosis), a gram-positive short rod that can cause similar changes to this case.[3,4,8]

Gram stain of the heart and lungs revealed intravascular gram-positive pairs and chains of cocci in thrombi, consistent with streptococcal infection. Consistent with non-aerogenous extra-pulmonary bacterial etiology, bacteria were not evident in airways. PCR on formalin-fixed tissues was positive for Group B *Streptococci* (GBS).

GBS are commensal bacteria residing in the urogenital, respiratory, and intestinal tract and can be associated with opportunistic infections, particularly in neonates and immunosuppressed individuals.[6] Most notably, maternal colonization of GBS in humans is a risk factor for neonatal meningitis, septicemia, pneumonia, and death. However, GBS infection in gravid rats is reported to cause multi-systemic lesions (suppurative pan-carditis, splenitis, pancreatitis, interstitial pneumonia, metritis, and bacterial thromboemboli) in the dam, with suppurative urocystitis as the possible source.[3] Uterovaginal origin also seems likely post-partum, however these tissues were unremarkable in our case.

GBS were among the most commonly identified bacteria in rat specimens (2016-2020 PCR results) in a recent report, with approximately 20% prevalence.[1] FELASA 2014 recommends quarterly monitoring for GBS in rats.[7] GBS is frequently excluded from routine health monitoring in laboratory rodents.[5] This case highlights a potentially important cause of morbidity in breeding colonies.

Contributing Institution:
Johns Hopkins University
School of Medicine
Department of Molecular & Comparative Pathobiology
https://mcp.bs.jhmi.edu/

JPC Diagnoses:
1. Heart: Endocarditis, myocarditis, and valvulitis, chronic-active, suppurative, diffuse, with septic thrombus, granulation tissue, and numerous cocci.
2. Lung, pulmonary arteries: Arteritis, necrotizing, multifocal, severe, with septic thrombi and numerous cocci.

JPC Comment:
Group B *Streptococci*, also known as *Streptococcus agalactiae*, are opportunistic bacteria that are estimated to colonize the gastrointestinal and urogenital tracts of 1 in 4 humans.[3] GBS are divided into 10 different serotypes based on the composition of their polysaccharide capsules, with different serotypes causing more or less virulent disease with implications for patient prognosis. Invasive GBS infection is causing growing levels of mortality and morbidity among neonates,

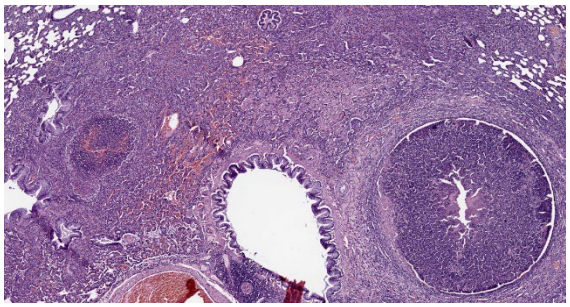

Figure 3-5. Lung, rat. Septic thrombi are also present within pulmonary arteries. The adjacent alveoli are atelectatic, and some contain various combinations and concentrations of neutrophils, cellular debris, and polymerized fibrin. (HE, 155X)

pregnant women, the elderly, and those with underlying health conditions. Invasive GBS infections have also been reported in primates, dogs, fish, and cattle, and rodents and primates have been used as experimental models of infection both neonatal and adult GBS infection.[3]

In laboratory rats, case reports of spontaneously occurring GBS infections often recapitulate late-onset GBS infections in humans, with infections characterized by myocarditis, metritis, meningitis, and septicemia.[3] Comparative phylogenetic analyses from animals as diverse as tilapia, cattle, and humans show that GBS strains are extremely closely related, and thus could represent an anthropozoonotic risk. Whether such trans-species transmission actually occurs is an active area of research; in the meanwhile, personal protective equipment and training on preventive measures for laboratory animal handlers is recommended.[3]

Discussion of this case centered initially on cardiac anatomy, with conference participants divided on whether the cardiac thrombus was located in the right or the left side of the heart. Dr. Alves noted that sequelae of a left-sided thrombus would be widely dissementated thrombus formation, while right sided thrombi might be expected to propagage clots within the pulmonary vasculature, as seen in this case. Duly convinced that the thrombus likely began in the heart, partipants noted the multiple small caliber blood vessels in the myocardium, particularly at the apex of the heart, and agreed with the contributor that, while a surprising location, these likely represented granulation tissue subjacent to the completely denuded endocardium.

Gram staining highlighted the embolic nature of this disease process, with large colonies of gram-positive bacteria throughout the pulmonary vasculature. The moderator also noted the substantial interstitial pneumonia present in the lungs and characterized the infiltrate as primarily lymphoplasmacytic with fewer neutrophils using immunohistochemical staining, including a stain for myeloperoxidase (MPO), which helpfully highlighted neutrophils.

Dr. Alves discussed coagulation more broadly, revisiting Virchow's triad of turbidity, endothelial damage, and hypercoagulability. In this case, the animal had recently given birth, and the hormonal changes associated with pregnancy and periparturition are known risk factors for hypercoagulability. The inflammatory conditions created by the massive bacterial infection could also cause vascular changes leading to slowing of blood flow and endothelial damage which could contribute to turbidity and exposure of tissue factor, all of which increase the risk of thrombus formation.

Conference participants preferred not to include the notable interstitial pneumonia in the

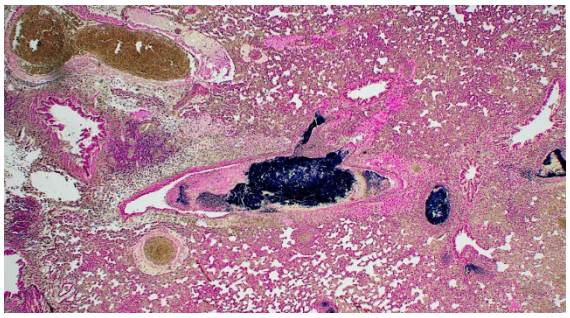

Figure 3-6. Lung, rat. Colonies of cocci within the pulmonary arteriolar thrombi are gram-positive. (Brown-Hopps, 100X)

morphologic diagnoses as it was likely secondary to the main process; however, the interstitial pneumonia was seen, acknowledged, and appreciated. Conference participants discussed the thrombus location within the heart at length, particularly whether it was located in the atrium or the ventricle. Participants noted the contributor's location of right atrium, which is undoubtedly correct; however, based on the slide evaluated at conference, participants could not definitively localize the thrombus and hedged with a generally correct location of "heart."

References:

1. Albers TM, Henderson KS, Mulder GB, Shek WR. Pathogen prevalence estimates and diagnostic methodology trends in laboratory mice and rats from 2003 to 2020. *JAALAS*. 2023;62(3):229-242.
2. Barthold SW, Griffey SM, Percy DH. *Pathology of Laboratory Rodents and Rabbits.* 4th ed. Blackwell Publishing; 2016.
3. Bodi Winn C, Bakthavatchalu V, Esmail MY, et al. Isolation and molecular characterization of group B *Streptococcus* from laboratory Long-Evans rats (*Rattus norvegicus*) with and without invasive group B streptococcal disease. *J Med Microbiol*. 2018;67(1):97-109.
4. Cooper TK, Meyerholz DK, Beck AP, et al. Research-relevant conditions and pathology of laboratory mice, rats, gerbils, guinea pigs, hamsters, naked mole rats, and rabbits. *ILAR J.* 2021;62(1-2):77-132.
5. Hansen AK, Nielsen DS, Krych L, Hansen CHF. Bacterial species to be considered in quality assurance of mice and rats. *Lab Anim*. 2019;53(3):281-291.
6. Mähler C, Berard M, Feinstein R, et al. FELASA recommendations for the health monitoring of mouse, rat, hamster, guinea pig and rabbit colonies in breeding and experimental units. *Lab Anim.* 2014; 48(3):178-192.
7. Otto GM. Chapter 4 - Biology and Diseases of Rats. In: *Laboratory Animal Medicine.* 3rd ed. Boston Academic Press; 2015.
8. Shuster KA, Hish GA, Selles LA, et al. Naturally occurring disseminated group B streptococcus infections in postnatal rats. *Comp Med*. 2013 Feb;63(1):55-61.

CASE IV:

Signalment:
Age and gender unknown, Sprague Dawley rat (*Rattus norvegicus*)

History:
The patient was enrolled in an IACUC protocol. Following surgery, the rat was not grooming, was urinating on itself, was very lethargic, and lost more than 15% of its body weight. There was no sign that it was eating food or gel packs. Euthanasia was performed and a necropsy was performed by the research technician.

Figure 4-1. Kidney, rat. Uroliths collected from the bladder. There was blood in the urine and culture of the urine yielded *Proteus mirabilis. (Photo courtesy of* Tri Service Research Laboratory, http://www.wpafb.af.mil /afrl/711HPW/)

Gross Pathology:
The bladder was distended and discolored. Urine collected aseptically was purulent and bloody. The stomach was full, but the rest of the gastrointestinal tract was empty. Both kidneys had multifocal white spots on the cortex. The remaining organs appeared normal. Gross dissection of the bladder revealed numerous uroliths.

Laboratory Results:
Proteus mirabilis was cultured from the urinary bladder. Stone analysis was not performed.

Microscopic Description:
Affecting 40% of primarily the renal cortex, but extending into the medulla, tubules are necrotic and degenerate, lost and replaced, or expanded and widely separated by viable and degenerate neutrophils, necrotic cellular debris (lytic necrosis) and large colonies of basophilic bacterial rods. Tubules are degenerate or regenerating. Multifocally tubules have retention of cellular architecture and loss of differential staining (coagulative necrosis). Within tubules there is a homogenous eosinophilic material (proteinosis) or sloughed epithelium admixed with neutrophils and cellular debris (cellular cast) and rarely deeply basophilic crystalline material (mineral). The interstitium is expanded by the same cellular debris and fibrin, hemorrhage and edema. Glomerular changes include synechia, parietal cell hypertrophy, necrosis of mesangial cells and protein in Bowman's space.

The renal surface is undulant with a mildly thickened capsule expanded by adherent fibrin and inflammatory cells. The renal pelvis is dilated (hydronephrosis) and contains previously described lytic necrosis and inflammatory cells which transmigrate the multifocally lost and necrotic (ulcerated) urothelium.

Contributor's Morphologic Diagnosis:
Kidney: Pyelonephritis, suppurative, multifocal, severe, chronic, with large colonies of bacteria, tubular degeneration, regeneration and necrosis, protein and cellular casts, intratubular bacteria, hydronephrosis, and urethritis.

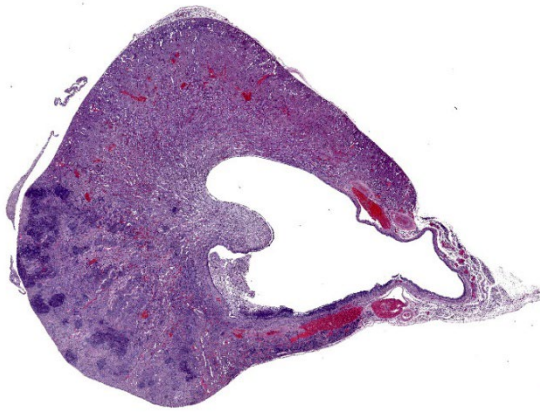

Figure 4-2. Kidney, rat. At subgross magnification, the renal pelvis is markedly dilated and irregular in shape. There is exudate in the lumen and foci of inflammation extending up to the undulant capsular surface. (HE, 6X)

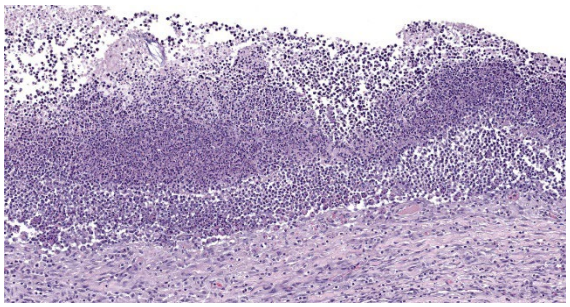

Figure 4-3. Kidney, rat. There is intense suppurative inflammation adjacent to ulcerated areas of the dilated pelvis. (HE,170X)

Contributor's Comment:
Proteus mirabilis is a gram-negative, flagellated, swarming, commensal inhabitant of the intestinal tract in humans and the respiratory and digestive tract of mice.[5] This bacteria may affect multiple organs by gaining access to the systemic circulation, inducing bacteremia, or can infect the urinary system through an ascending infection. In people, this is a common nosocomial cause of catheter associated urinary tract infections. In the dog and cat, *Escherichia coli* followed by *Proteus mirabilis* are the two most frequently isolated gram negative bacteria in urinary tract infections.[3] On a more historic note, *P. mirabilis* has been a source of surgical infection via contaminated instrumentation and has rarely been implicated in cases of meningitis and cerebral abscesses in neonates.[8]

The pathogenesis of *P. mirabilis* involves its unique ability to differentiate from a swimmer cell to a swarmer cell depending on the environment. In a liquid environment, the bacteria swim, (called swimmers) while on a solid surface, such as a urinary catheter, they differentiate into swarmers forming rapidly moving rafts of bacteria.[2] *P. mirabilis* has several virulence factors, including flagella for increased motility, adhesion factors for binding to epithelium in the urinary tract, and the ability to utilize host iron.[1,2] This infection also creates an overwhelming neutrophilic response and damages host tissue via hemolysin, which is cytotoxic to epithelial cells, and urease. Urease breaks down urea to ammonia, raising the pH of the urine and precipitating the formation of stones which are often struvite or carbonate hydroxyapatite, thus causing additional mechanical epithelial damage.[1,2]

One current area of research has been the investigation of *P. mirabilis* and its potential to alter tumor hypoxia thereby inhibiting tumor growth.[9] Through various mechanisms, such as gene delivery and immunomodulator delivery, *Salmonella typhimurium, E. coli* and *Clostridium* sp. have also been investigated for their potential roll in treating cancer.[7] One particular study found that *P. mirabilis* may be a potential method for suppressing growth of primary breast cancer in murine models.[9]

Although not a common pathologic entity in veterinary medicine, this bacteria should be considered as a differential for cases of suppuarative pyelonephritis in rodents.

Contributing Institution:
Tri Service Research Laboratory
Fort Sam Houston, TX
http://www.wpafb.af.mil/afrl/

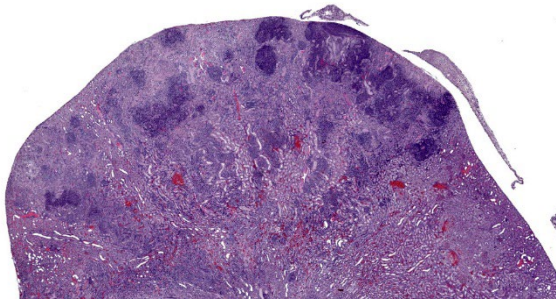

Figure 4-4. Kidney, rat. Rays of inflammation extend upward into the superficial cortex. (HE,17X)

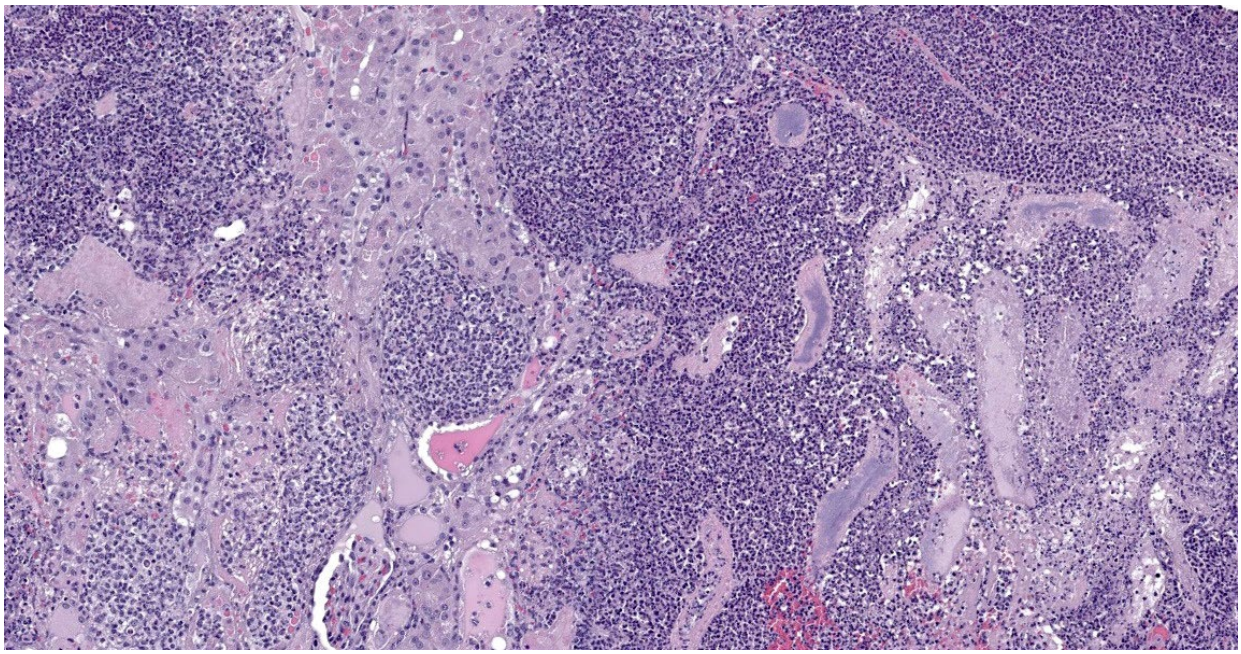

Figure 4-5. Kidney, rat. Tubules are expanded and effaced by suppurative inflammation which extends into the surrounding interstitium. Some tubules contain protein casts filled with apparent bacterial colonies. (HE,144X)

JPC Diagnoses:

1. Kidney: Pyelonephritis, chronic-active, suppurative, severe, multifocal to coalescing, with cellular and protein casts and moderate hydronephrosis.
2. Kidney: Interstitial nephritis, lymphoplasmacytic, mild, with tubular atrophy.

JPC Comment:

The contributor provides an excellent overview of *Proteus mirabilis*, a bacterium blessed with many gifts, the most spectacular of which may be its remarkable and pleasingly alliterative swimmer-swarmer motility. This unique feature inspired the name of the *Proteus* genus upon its discovery in 1885 by the German pathologist Gustav Hauser.[7]

Hauser, a Greek mythology enthusiast, named the genus based on Proteus, the prophetic sea god, who appears in, among other writings, Homer's *Odyssey*. In addition to herding seals for Poseidon – a fine enough avocation in itself – Proteus was omniscient, knowing all things past, present, and future. Proteus was loathe, however, to share his knowledge with others, and those who sought his counsel could only bide their time and attempt to capture Proteus during his midday nap and demand prophetic answers. Proteus, however, was not just your run-of-the-mill omniscient seal-herding deity; he could also change shape into lions, serpents, or even water in order to avoid capture.

The name Proteus also appeared in the 15th century Shakespeare play, *The Two Gentlemen of Verona*, where one of the main characters is so named because of his capricious, frequently-changing affections. The modern word "protean" also shares this derivation, and is defined by Merriam-Webster to mean "of or resembling Proteus in having a varied nature or ability to assume different forms; displaying great diversity or variety; versatile."[9] It was this culture context that led

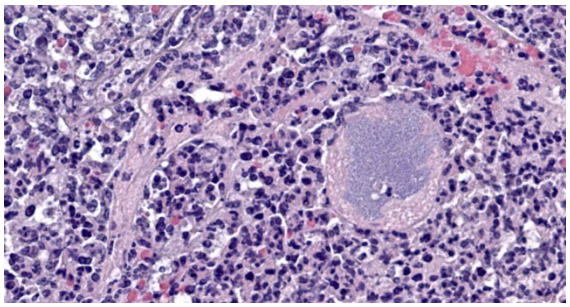

Figure 4-6. Kidney rat. High magnification of the granular material within the lumen of a dilated tubule in the superficial cortex. (HE, 914X)

Hauser, who recognized the ability of *Proteus mirabilis* to differentiate from a short vegetative swimmer cell to an elongated, highly flagellated swarmer cell, to name the bacterium after Proteus, mythology's famous shape-shifter.[8]

What Hauser couldn't have know at the time, however, is that *P. mirabilis* can perform even more feats of molecular chicanery that allow it to evade the host immune system. *P. mirabilis* produces an IgA-degrading protease, named ZapA metalloprotease, that is able to completely degrade IgA.[1] The bacterium produces ZapA during its transition from swimmer to swarmer, enabling it to neutralize the host's mucosal immunity during a critical time in pathogenesis. One of the key characteristics of the swarmer cell is the exuberant expression of flagella of many different types. These flagella are encoded by three different flagellin genes which, via homologous recombination, allow individual bacteria to produce antigenically novel flagella capable of evading host immune defenses.[1] Finally, the production of urease leads to the production of struvite and carbonate hydroxyapatite stones. Stone formation is typical of *P. mirabilis* infection and allows the bacterium to sequester itself and replicate within the stones, protected from the antibodies and antibiotics that mean it harm.[1] Conference participants found this slide a feast for the eyes and, as in all cases this week, full of description-rich details. Dr. Alves advised conference participants to structure slide descriptions by starting with the most severe lesion; if severity doesn't provide an obvious starting point, one might structure the description around the presumed pathogenesis. In this case, the most severe pathology was in cortical tubules, which were characterized by large areas of both coagulative and lytic necrosis. Dr. Alves noted that many seemingly destroyed tubules retained their basement mebranes in a remarkable display of renal resilience. He also noted that many tubular lumina contain blue-gray, finely granular material that appear to be bacteria, but that did not show up on gram stain. Gram staining was repeated post-conference and the intratubular material again resisted gram staining. Despite the presence or absence of organisms on gram stain, this section provides an excellent example of a "gram-negative kidney," with lesions similar to what would be expected with *E. coli*, *Proteus mirabilis*, *Klebsiella*, and other less-common gram negative organisms.

Dr. Alves also noted eosinophilic round inclusions within many renal tubular epithelial cells, interpreted as hyaline droplets. These well-documented droplets are produced by one of three distinct processes: 1) by sequestration of alpha2U-globulin in the lysosomes of male rats, 2) by histiocytic sarcoma, which produces excessive lysozyme that spills into the renal tubules and is resorbed, or 3) by overproduction of high molecular weight proteins. These three etiologies can only be differentiated with special stains.

Finally, Dr. Alves noted an area near the renal pelvis that, in contrast to the vast majority of the kidney which is awash in neutrophils, contains an interstitial inflammatory infiltrate composed largely of lymphocytes and plasma cells. These chronic inflammatory cells separate and surround small renal tubules with attenuated epithelium, interpreted as tubular atrophy. Dr. Alves believes this area represents a second pathologic process distinct from the obvious bacterial infection. Though the age of the animal is not provided, chronic progressive nephropathy is a common lesion in older rats and could account for this focus of chronic inflammation. Conference participants felt this was a significant lesion and warranted capture in a second morphologic diagnosis.

References:

1. Coker C, Poore CA, Li X, Mobley HLT. Pathogenesis of *Proteus mirabilis* urinary ratct infection. *Microbes Infect.* 2000; 2(12):1497-1505.
2. Jones B, Young R, Mahenthiralingam E, Stickler D. Ultrastructure of *Proteus mirabilis* swarmer cell rafts and role of swarming in catheter-associated urinary tract infection. *Infect Immun.* 2004; 72 (7):3491-3950.
3. Marques C, Belas A, Franco A, Aboim C, Gama LT, Pomba C. Increase in antimicrobial resistance and emergence of major international high-risk clonal lineages in dogs and cats with urinary tract infection: 16 year retrospective study. *J Antimicrob Chemother*. 2018;73(2):377-384.
4. Mobley HLT. Virulence of *Proteus mirabilis*. In: Mobley H, Warren J, eds. *Urinary Tract Infections: Molecular Pathogenesis and Clinical Management.* ASM Press;1996:245-269.
5. Percy DH, Barthold SW, eds. *Pathology of Laboratory Rodents and Rabbits.* 4th ed. Blackwell Publishing; 2016:66.
6. Protean. 2023. In:*Merriam-Webster.com.* Retrieved December 9, 2023, from https://www.merriam-webster.com/dictionary.
7. Sellaturay SV, Nair R, Dickinson IK, Sriprasad S. Proteus: mythology to modern times. *Indian J Urol*. 2012;28(4):388-391.
8. Smith ML, Mellor D. *Proteus mirabilis* meningitis and cerebral abscess in the newborn period. *Arch Dis Child.* 1980; 55(4):308-310.
9. Zhang H, Diao H, Jia L, Yuan Y, Thamm D et al. Proteus mirabilis inhibits cancer growth and pulmonary metastasis in a mouse breast cancer model. *PLoS One.* 2017;12(12):e0188960.